Effects of the uncertainties of climate change on the performance of hydropower systems

Babak Zolghadr-Asli, Omid Bozorg-Haddad and Xuefeng Chu

ABSTRACT

This study's objective is to assess the potential impact of climate change on an example under-design hydropower system in the Karkheh River basin, Iran. Based on three water resources performance criteria (reliability, resiliency, and vulnerability), a novel framework was proposed to interpret and cope with the uncertainties associated with such assessments. The results demonstrated the acceptable performance of the system in most months, while there were certain signs for rare low-inflows, and consequently low hydropower generated by the system, due to the climate change. It was found that in terms of these three criteria, the best performances in the climate-change condition occurred in May (80% reliability), December (45% resiliency), and April (19% vulnerability). Yet the worst performances occurred in September (2% reliability), July and August (0% resiliency), and in October (39% vulnerability). These results indicated that the reliability and resiliency of the system would be improved under the climate change condition, while due to the increase of low-inflow incidences, the vulnerability of the system would increase. This suggests that, although the system may not face frequent failures, severe blackouts may occur. With timely consideration of future climatic conditions and appropriate adaptive actions, including additional backup systems for reliable and safe electricity generation, future undesired conditions can be avoided in the basin.

Key words | climate change, hydropower generation, performance criterion, reservoir operation, uncertainty, water resources management

Babak Zolghadr-Asli
Omid Bozorg-Haddad (corresponding author)
Department of Irrigation & Reclamation Engineering, Faculty of Agricultural Engineering & Technology, College of Agriculture & Natural Resources,
University of Tehran,
3158777871 Karaj,
Iran
E-mail: *obhaddad@ut.ac.ir*

Xuefeng Chu
Department of Civil & Environmental Engineering,
North Dakota State University,
Department 2470, Fargo, ND,
USA

INTRODUCTION

While the world's population growth must become a major concern, constant improvements in the welfare and lifestyle of the residents of the 'blue planet' may have caused over-exploitation of many natural resources (Singh *et al.* 2014). Non-renewable energy resources fit the descriptions to be listed in such a category. Modern civilizations require a substantial amount of energy resources. As a result, many communities are currently facing difficulties in meeting such demands. Reportedly, in 2014, the world's total primary energy supply (TPES) was estimated to be 13,699 Mtoe, which showed an increase of 2.45% compared to 2012. According to the International Energy Agency, some 81% of the global TPES was met by tapping into fossil fuels (coal, oil, and natural gas) (IEA 2016). The represented values are expected to escalate dramatically in the foreseeable future, due to the positive trend in population growth and continuing consumption of natural fuel resources (Dincer & Acar 2015), especially given that a higher rate of population growth is projected for urban areas, which may also have a higher rate of energy demand per capita (Vörösmarty *et al.* 2000). Nevertheless, the process of fossil fuel formation takes millenniums, thus making them limited or

doi: 10.2166/wcc.2018.120

non-renewable resources (Halbouty 1990). In addition to the adverse impacts of such energy resources on the environment, given the fact that the global energy market (one of the most influential financial markets of the world) is currently dominated by such resources (Shafiee & Topal 2009), the world's economy may be greatly injured by any downturn in the market of fossil fuels (Dincer & Acar 2015). Subsequently, these resources cannot be considered as a long-term and sustainable solution to the rising demand for energy sources. Thus, searching for an alternative energy resource may seem a logical, yet inevitable, approach. These alternative resources should not only be easily accessible throughout the world, but must also have the least adverse environmental impacts (e.g. emission of greenhouse gases). Additionally, these alternative resources can be categorized as renewable resources.

Currently, the most viable and environmentally friendly resources that could be considered as an alternative to fossil fuels are solar, wind, ocean, hydropower, biomass, and geothermal energy. However, among the proposed alternative energy resources, some may have more suitable characteristics. Solar and wind energy, for instance, have an intermittent and fluctuating nature, and to ensure a steady energy generation, additional backup systems may be required. However, hydropower plants, due to their unique nature, may be a more suitable choice than others. Accounting for nearly 20% of electricity production worldwide, hydropower is, by far, the most suitable renewable energy source (Dincer & Acar 2015). Future energy market predictions projected that this resource may remain as one of the most viable options, regardless of the future targets of energy markets in many countries (IPCC 2014a).

While hydropower has many advantages over traditional and most other renewable energy resources, it can also affect and be affected by any upcoming changes in both global or regional climate behaviors, due to its direct dependence on the magnitude and timing of streamflow. Therefore, the viability of hydropower projects at its current or planned status remains in question under the projected changes in the climatic behavior, and spatial and temporal streamflow changes associated with such phenomena (IPCC 2014a).

Loosely, the term 'climate change' refers to any change in the long-term average or extreme climatic behavior of a region. While climate change projections demonstrate a positive trend in the average global temperature (IPCC 2014a, 2014b), such a decisive statement does not imply any regional scale behaviors of the temperature or any other climatic variables. Evidently, these changes may exacerbate the situation of water resources in arid and semi-arid regions, including the Middle East and North African nations, which, needless to say, are already experiencing mild to severe water stress due to the limited water availability and growing water demands (Sowers *et al.* 2011). Although the viability of hydropower projects coincide with these upcoming changes in the climate, mitigation and adaptive measurements do not have high priority in these nations (Sowers *et al.* 2011), in which aggressive development plans rely solely on historical rather than climate change conditions. This may be due to the fact that climate change is tied with numerous uncertain projections, which may add complexity to an already complex problem.

In fact, the basic core of any scientific research is striving for an objective perspective. Yet, inevitably, there will be some cases in any scientific assessment which may require unbiased adept choices. In climatic sciences, for instance, such decisions may revolve around the adaptation of global circulation models (GCMs), downscaling techniques, hydrological models, and other such matters. Due to the fact that in many of these cases there is no specific advantage or logical priority over a variety of possible options that can produce feasible results, such choices are considered as sources of uncertainty (Zolghadr-Asli 2017). The concept of uncertainty is an insuperable characteristic of natural phenomena's behavioral pattern predictions. Such a lack of certainty originated either from the lack of information (aleatoric uncertainty) or the nature of the phenomenon (epistemic uncertainty). It is common to partition the uncertainty surrounding climate change into four main categories: (1) scenario uncertainty; (2) model uncertainty; (3) internal variability and initial condition uncertainty; and (4) forcing and boundary condition (Collins & Allen 2002; Yip *et al.* 2011). Such uncertainties can generate numerous feasible projections for climatic behavior in both regional and global scales, which in turn can affect the anticipated performance of hydropower projects.

Given the indispensable role of hydropower in both developing and developed nations, comprehensive studies are required to shed light on the plausible impacts of climate change on the performances of hydropower projects. Consequently, numerous studies were aimed at assessing hydropower generation under the climate change condition (e.g. Switzerland (Westaway 2000; Schaefli *et al.* 2007), Sweden (Bergström *et al.* 2001), the Colombia River basin (Payne *et al.* 2004), the Colorado River basin (Christensen *et al.* 2004), California (Medellín-Azuara *et al.* 2008; Vicuña *et al.* 2008; Connell-Buck *et al.* 2011; Guégan *et al.* 2012), Canada (Minville *et al.* 2009, 2010), Scotland (Sample *et al.* 2015), Brazil (Prado *et al.* 2016), China (Liu *et al.* 2016), India (Chandel *et al.* 2016), Portugal (Teotónio *et al.* 2017), and the Niagara River basin (Meyer *et al.* 2017)). As evidenced by the aforementioned literature review, while most developed nations are consistently updating their climate change estimations and the plausible impacts of such changes on the performances of hydropower projects, most developing nations, including but not limited to the Middle Eastern countries, either completely ignore the impact of climate change on hydropower projects or fail to update their climate change projections in such assessments. Subsequently, while developed nations can devise mitigation and adaptation plans for their ongoing hydropower projects, most hydropower projects in developing nations may be based on either overestimated streamflow (climate change exacerbates the water resources conditions and the projects cannot work with the full design capacity), or underestimated streamflow (climate change improves the water resources conditions and the projects fail to harness the full potential of the regions' capacity for hydropower generation) (IPCC 2014b).

The main objective of this study is to propose a framework through which the decision-makers are able to interpret and analyze the potential impact of climate change on hydropower and evaluate the uncertainties that are associated with such assessments. With ease of use and, relatively, fewer computational requirements, the proposed approach, which is based on the water resources performance criteria, can help the water resources decision-makers to cope with uncertainties associated with hydropower systems and climate change. To demonstrate the aforementioned framework, the Karkheh River basin hydropower system in Iran was selected. The climate change scenarios of the fifth assessment report (AR5) of the IPCC, namely representative concentration pathways (RCPs), were used. The datasets from the second generation of the Canadian Earth System Model (CanESM2) were downscaled using both the change factor technique and the statistical downscaling model (SDSM). The 4-reservoir hydropower system (Sazbon-e Jariani, Sazbon-e Makhzani, Seimareh, and Karkheh Jariani reservoirs) was simulated under both baseline and climate change conditions. The uncertainties associated with the results were then evaluated using the central tendency (mode, median, and average) and disperse indicators (range, standard deviation, and skewness), as well as a framework which was based on the probability-based performance criteria (PBPC), in terms of reliability, resiliency, and vulnerability.

MATERIALS AND METHODS

This section discusses the data processing procedures required for constructing climatic scenarios, transforming the generated climatic scenarios into hydrological data, and finally simulating the hydropower systems and analyzing the uncertainties associated with the produced results. The basic steps of the proposed procedures are schematically shown in Figure 1.

Construction of climate scenarios

Constructing the climate scenarios is based upon three major steps. The initial step is to introduce the assumptions regarding the future behavior of climatic drivers. Such scenarios are designed to ease the assessment for future developments of complex systems that are either inherently unpredictable, or are associated with high scientific uncertainties. For years, emissions scenarios from the 'special report on emissions scenarios' (SRES) (IPCC 2007) were used as the main source for exploring uncertainties from anthropogenic climate drivers. However, a new concept called Representative Concentration Pathways (RCPs) (Van Vuuren *et al.* 2011) has been proposed and used in recent studies.

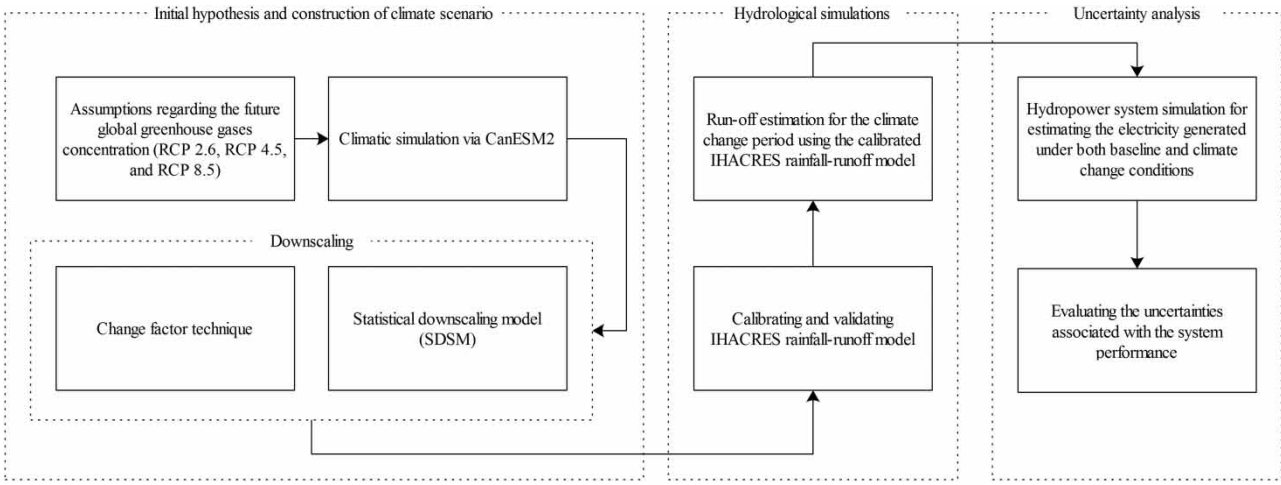

Figure 1 | Flowchart of the proposed methodology.

RCPs are newly defined scenarios that specify the concentrations of greenhouse gases and their plausible emission patterns. However, unlike the previous IPCC's emission scenarios, they are not directly centered around socio-economic storylines, but rather based on a different approach that includes more consistent short-lived gases and land use changes (IPCC 2013). In fact, the term 'RCPs' is deliberately chosen to emphasize that these trajectories are not definitive emission scenarios, but rather sets of time-dependent forcing projections that could potentially represent more than one underlying socio-economic scenario (Van Vuuren *et al.* 2011; Zolghadr-Asli 2017).

RCPs are identified by the approximate values of their radiative forcing (RF) (W/m^2). RCP 2.6, which represents the most optimistic projection compared to the four most common RCPs, peaks at 3.0 W/m^2 and then declines to 2.6 W/m^2 by the year 2100. RCP 4.5 and RCP 6.0, which represent moderate projections for upcoming changes in the climate, stabilize after 2100 at 4.2 and 6.0 W/m^2, respectively; while RCP 8.5, which is the most pessimistic climate change projection, reaches 8.3 W/m^2 in 2100 on a rising trajectory (IPCC 2013). Ultimately, the primary objective of these scenarios is to provide all input data necessary to run comprehensive climate models. Note that due to the substantial uncertainties in RF trajectories, these forcing values represent comparative *markers*, rather than the exact forcing values.

The second step for constructing the climate scenarios is to simulate the global climatic behavior in response to the assumed RCPs by using CanESM2. CanESM2 integrates an atmosphere-ocean general circulation model, a land-vegetation model, and five terrestrial and oceanic interactive carbon cycles (Chylek *et al.* 2011a). The results of adopting this model in various climate studies have demonstrated its model's potential, given the considerable improvement in its simulation results compared to the earlier versions of the CanCM3 and CCSM3 models. For instance, Chylek *et al.* (2011a) explored the application of CanESM2 and its potential weakness and strengths in the global climatic simulation. Although they were able to demonstrate the vast capabilities of this model for the global climatic simulation, they were unable to conclusively pinpoint the reason behind this advantage. However, such a model improvement can probably be attributed to more realistic treatment of atmospheric aerosols (Mishchenko *et al.* 2010), surface use changes (Pielke *et al.* 2002, 2007), and introduction of clouds in the simulation process (Polyakov & Johnson 2000; Dijkstra *et al.* 2006; Chylek *et al.* 2011a, 2011b). Note that CanESM2 uses a Gaussian 128×64 grid to simulate the earth's climatic behavior. The resolution of this model is (2.8°, 2.8°) (longitude, latitude) for the atmosphere, and (1.4°, 1.4°) (longitude, latitude) for the ocean (Chylek *et al.* 2011a, 2011b).

Chiefly, GCM projections use a large-scale computational grid (resolution) in terms of time and space, which resultantly reduces the accuracy of the generated results

for most regional study areas. There are also techniques available for downscaling the GCM outputs to a specific region or study area of interest. Consequently, the final step in the climate construction procedure is spatial, or in some cases even temporal, downscaling of the GCM outputs. Among numerous methods available for downscaling climatic data, weather typing approaches involve grouping local meteorological data in order to prevail patterns of atmospheric circulation. Weather pattern downscaling, generally speaking, is founded on sensible linkages between climate on the large scale and weather at the local scale. This family of techniques is also applicable to a wide variety of environmental variables, as well as multi-site applications (Wilby & Dawson 2007).

The change factor technique is utilized for simple spatial downscaling (Adhikari *et al.* 2016). In this simple weather typing approach, the climate scenarios are obtained by computing the differences (or ratio, depending on the nature of the climate variables) between the averages of the GCM dataset for the climate change period and the corresponding averages of the model's simulation results for the baseline period. The changes in air temperature are usually expressed as differences, whereas for rainfall changes, ratios are commonly used (Wilby & Harris 2006; Adhikari *et al.* 2016). The air temperature and rainfall changes in the change factor downscaling procedure can be expressed as:

$$\Delta T_i = \bar{T}_i^{fut} - \bar{T}_i^{base} \tag{1}$$

$$\Delta P_i = \frac{\bar{P}_i^{fut}}{\bar{P}_i^{base}} \tag{2}$$

$$T_i = T_i^{obs} + \Delta T_i \tag{3}$$

$$P_i = P_i^{obs} \times \Delta P_i \tag{4}$$

in which ΔT_i and ΔP_i = average long-term monthly air temperature and rainfall changes for month i, respectively; $\bar{T}_i^{fut}$ and $\bar{P}_i^{fut}$ = average long-term monthly air temperature and rainfall for month i simulated by the GCM for the climate change period, respectively; $\bar{T}_i^{base}$ and $\bar{P}_i^{base}$ = average long-term monthly air temperature and rainfall for month i simulated by the GCM for the baseline period, respectively; T_i^{obs} and P_i^{obs} = observed air temperature and rainfall for month i, respectively; and T_i and P_i = air temperature and rainfall for month i in the climate change period, respectively.

Although the simplicity of the change factor technique is to be considered as an advantage, and in fact such ease of calculation does not necessarily induce errors in the procedure of climate scenario construction, it should be noted that the weather typing schemes, in general, can have a parochial perspective on the downscaling procedure, due to a poor basis of downscaling rare extreme events, which has a tendency to depend on the stationary circulation-to-surface climate relationships. Potentially, the most serious limitation is that rainfall changes produced by changes in the frequency of weather patterns are seldom consistent with the changes produced by the host GCM (Wilby & Dawson 2007; Zolghadr-Asli 2017). Thus, it is advisable to couple the results of such methods with other approaches, to ensure the accuracy of the downscaling methods. Subsequently, the SDSM was additionally employed in this study to facilitate the rapid development of multiple, low-cost, and single-site scenarios of daily surface weather variables under the baseline and future regional climate forcing (Wilby *et al.* 2002). The accurate performance of SDSM, which loosely speaking can be described as a multi-regression, water generator downscaling model, has been tested in many studies (e.g. Hashmi *et al.* 2011; Meenu *et al.* 2013; Sobhani *et al.* 2016). For more information on the basic principle and applications of SDSM, readers can refer to Wilby *et al.* (2002) and Wilby & Dawson (2007).

Hydrological simulations: estimating the water resources conditions under climate changes

Hydrologic simulation is required to transform the constructed climatic scenarios into the hydrologic response to the climate change. IHACRES (identification of unit hydrographs and component flows from rainfall, evaporation, and streamflow data) is a lumped, semi-conceptual model (Jakeman & Hornberger 1993), which has been proven to be an efficient option for such a task (e.g. Hansen *et al.* 1996; Dye & Croke 2003; Abushandi & Merkel 2003). Perhaps one of the major advantages of the IHACRES

model over other commonly-used rainfall-runoff models (e.g. Chen *et al.* 2015; Taormina *et al.* 2015; Wang *et al.* 2015) is its minimal input data requirement (air temperature and rainfall) (Jakeman & Hornberger 1993). Basically, the IHACRES is composed of two modules: (1) a non-linear loss module, which converts the observed rainfall into the effective rainfall; and (2) a linear unit hydrograph module, which, in essence, converts the effective rainfall into the simulated streamflow (Jakeman & Hornberger 1993) (Figure 2).

Naturally, the IHACRES model needs to be calibrated and validated. The three quantitative statistical parameters used to evaluate the performances of the IHACRES model include: Nash–Sutcliffe efficiency (*NSE*) coefficient (Nash & Sutcliffe 1970), percent bias (*PB*) (Gupta *et al.* 1999), and ratio of root-mean-square error (*RMSE*) to observations standard deviation (*RSR*) (Moriasi *et al.* 2007), which are respectively given by:

$$NSE = 1 - \left[\frac{\sum_{t=1}^{N}(x_t^{obs} - x_t^{sim})}{\sum_{t=1}^{N}(x_t^{obs} - x_{mean}^{obs})}\right] \quad (5)$$

$$PB = \left[\frac{\sum_{t=1}^{N}(x_t^{obs} - x_t^{sim})}{\sum_{t=1}^{N} x_t^{obs}}\right] \times 100 \quad (6)$$

$$RSR = \left[\frac{\sqrt{\sum_{t=1}^{N}(x_t^{obs} - x_t^{sim})^2}}{\sqrt{\sum_{t=1}^{N}(x_t^{obs} - x_{mean}^{obs})^2}}\right] \quad (7)$$

where x_t^{obs} and x_t^{sim} = observed and simulated streamflow in the tth time step, respectively; x_{mean}^{obs} = mean of the observed streamflow data; and N = number of time steps. *NSE* ranges from $-\infty$ to 1.0 (1.0 for a perfect fit); and *RSR* ranges from 0 to $+\infty$ (0 for a perfect fit) (Moriasi *et al.* 2007). For a monthly time step, a *PB* value between −25 and +25%, an *NSE* value greater than 0.5, or an *RSR* value less than or equal to 0.7 is considered satisfactory (Moriasi *et al.* 2007; Adhikari *et al.* 2016).

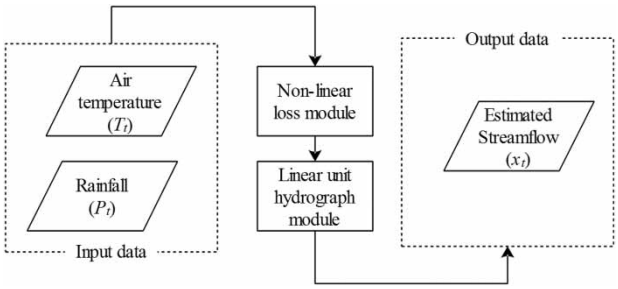

Figure 2 | Flowchart of the IHACRES model.

Hydropower simulation

Hydropower simulation, naturally, is the prerequisite step to quantify the impacts of climate change on a hydropower system. Modeling of a hydropower system includes simulations of both water and power, which can be respectively expressed as Equations (8)–(14) (for water) and Equations (15)–(18) (for power):

$$S_{(r,t+1)} = S_{(r,t)} + Q_{(r,t)} + M_{n\times n}Re_{(r,t)} - Sp_{(r,t)} - Loss_{(r,t)} \quad r = 1, \ldots, n\text{Res}; t = 1, \ldots, N \quad (8)$$

$$Loss_{(r,t)} = A_{(r,t)} \times Ev_{(r,t)} \quad r = 1, \ldots, n\text{Res}; t = 1, \ldots, N \quad (9)$$

$$A_{(r,t)} = G[S_{(r,t)}] \quad r = 1, \ldots, n\text{Res}; t = 1, \ldots, N \quad (10)$$

$$Sp_{(r,t)} = \frac{|\text{Smax}_r - AW_{(r,t)}| - [\text{Smax}_r - AW_{(r,t)}]}{2} \quad r = 1, \ldots, n\text{Res}; t = 1, \ldots, N \quad (11)$$

$$AW_{(r,t)} = S_{(r,t)} + Q_{(r,t)} + M_{nRes\times nRes}\text{Re}_{(r,t)} - Loss_{(r,t)} \quad r = 1, \ldots, n\text{Res}; t = 1, \ldots, N \quad (12)$$

$$0 \le \text{Re}(r, t) \le R\text{max}_r \quad r = 1, \ldots, n\text{Res}; t = 1, \ldots, N \quad (13)$$

$$Smin_r \le S_{(r,t)} \le \text{Smax}_r \quad r = 1, \ldots, n\text{Res}; t = 1, \ldots, N \quad (14)$$

$$PP_{(r,t)} = \frac{\gamma_W \times g \times \eta_r \times \Delta\text{H}_{(r,t)} \times Re_{(r,t)}}{86'400 \times Countday_t \times n_r} \quad r = 1, \ldots, n\text{Res}; t = 1, \ldots, N \quad (15)$$

$$\Delta H_{(r,t)} = H_{(r,t)} - TW_{(r,t)} \quad r = 1, \ldots, n\text{Res}; t = 1, \ldots, N \quad (16)$$

$$H_{(r,t)} = F[S_{(r,t)}] \quad r = 1, \ldots, n\text{Res}; t = 1, \ldots, N \quad (17)$$

$$TW_{(r,t)} = Y\left[Re_{(r,t)}\right] \quad r = 1, \ldots, n\text{Res}; t = 1, \ldots, N \tag{18}$$

in which $S_{(r,t)}$ and $S_{(r,t+1)}$ = stored water volume in the rth reservoir at the tth and $(t+1)$th time-step, respectively; $Q_{(r,t)}$ = upstream inflow volume to the rth reservoir at the tth time step; $M_{nRes \times nRes}$ = reservoirs' connection matrix; $Re_{(r,t)}$ = released water volume from the rth reservoir at the tth time step; $Sp_{(r,t)}$ = spilled water volume from the rth reservoir at the tth time step; $Loss_{(r,t)}$ = lost volume of water due to evaporation for the rth reservoir at the tth time step; $A_{(r,t)}$ = water surface area of the rth reservoir at the tth time step; $Ev_{(r,t)}$ = evaporation water depth of the rth reservoir at the tth time step; $G[]$ = simulating function of the stored water's surface area; $AW_{(r,t)}$ = available water in the rth reservoir at the tth time step; $Smax_r$ = storage capacity of the rth reservoir; $Rmax_r$ = maximum water volume released from the rth reservoir within a time step; $Smin_r$ = dead storage of the rth reservoir; $PP_{(r,t)}$ = generated hydropower by the rth reservoir at the tth time step; γ_W = water specific weight; g = gravitational acceleration; η_r = efficacy of the rth reservoir's hydropower system; $\Delta H_{(r,t)}$ = height difference between the reservoir water level and the tailwater level of the rth reservoir at the tth time step; $Countday_t$ = number of days within the tth time step; n_r = plant factor for the rth reservoir's hydropower system; $H_{(r,t)}$ = water level of the rth reservoir at the tth time step; $TW_{(r,t)}$ = height of downstream water for the rth reservoir at the tth time step; $F[]$ = simulating function of the water level; $Y[]$ = simulating function of the tailwater level; and $nRes$ = total number of reservoirs.

A common approach to manage withdrawal of the stored water is to establish seasonal targets for water level control. These predefined rules, i.e. rule curves (RCs), determine how the operator should behave at any given state of the reservoir (Zolghadr-Asli *et al.* 2016a). RCs are established as an attempt to balance various water needs such as flood control, hydropower, water supply, navigation, fish and wildlife habitat, recreation, and others (Mower & Miranda 2013). One of the most basic RCs is the standard operating policy (SOP). A SOP operating system attempts to release water given the water demand at the current step time, with no regards to the future. The SOP is basically designed to operate reservoirs with downstream demands (e.g. agricultural or municipal water demands). Figure 3 shows the flowchart of the hydropower system SOP, which is developed for reservoirs that are working in series.

Performance criteria

Various criteria have been applied to assess the performance of water resources systems. Such performance criteria are as simple as the average of a specific output or more complex entities such as the PBPC (Texas Commission on Environmental Quality 2007). It is common to tailor the performance criteria to specific objectives of a water system (Zolghadr-Asli *et al.* 2016b).

Hashimoto *et al.* (1982a, 1982b) pioneered the probability based performance assessment for water resources systems. Since the introduction of the PBPC, many studies have reviewed these criteria (e.g. Fiering 1982; Moy *et al.* 1986; Kundzewicz & Laski 1995; Srinivasan *et al.* 1999), and some researchers also proposed changes in their definitions (e.g. El-Baroudy & Simonovic 2004; Ermini & Ataoui 2013; Zolghadr-Asli *et al.* 2016b). However, the most fundamental and common PBPCs are resiliency, reliability, and vulnerability (RRV). Basically, reliability refers to the probability of a successful performance of a system; resiliency measures the probability of successful functioning, following failure of a system; and vulnerability quantifies the severity of the probable failures during the operation. While reliability and resiliency are dimensionless, vulnerability may have dimensionality.

According to the reliability criterion, the system state $[X_{(r,t)}]$ is divided into Success (S) and Failure (F). While each water resources system has unique definitions of success and failure, the state of a hydropower system can be defined as:

$$X_{(r,t)} = \begin{cases} 1 & if \quad PP_{(r,t)} = PPC_r \\ 0 & if \quad PP_{(r,t)} \neq PPC_r \end{cases} \quad r = 1, \ldots, n\text{Res}; t = 1, \ldots, N \tag{19}$$

Using the system state, the reliability of a hydropower system can be expressed as:

$$\alpha_r = \frac{\sum_{t=1}^{N} X_{(r,t)}}{N} \quad r = 1, \ldots, n\text{Res} \tag{20}$$

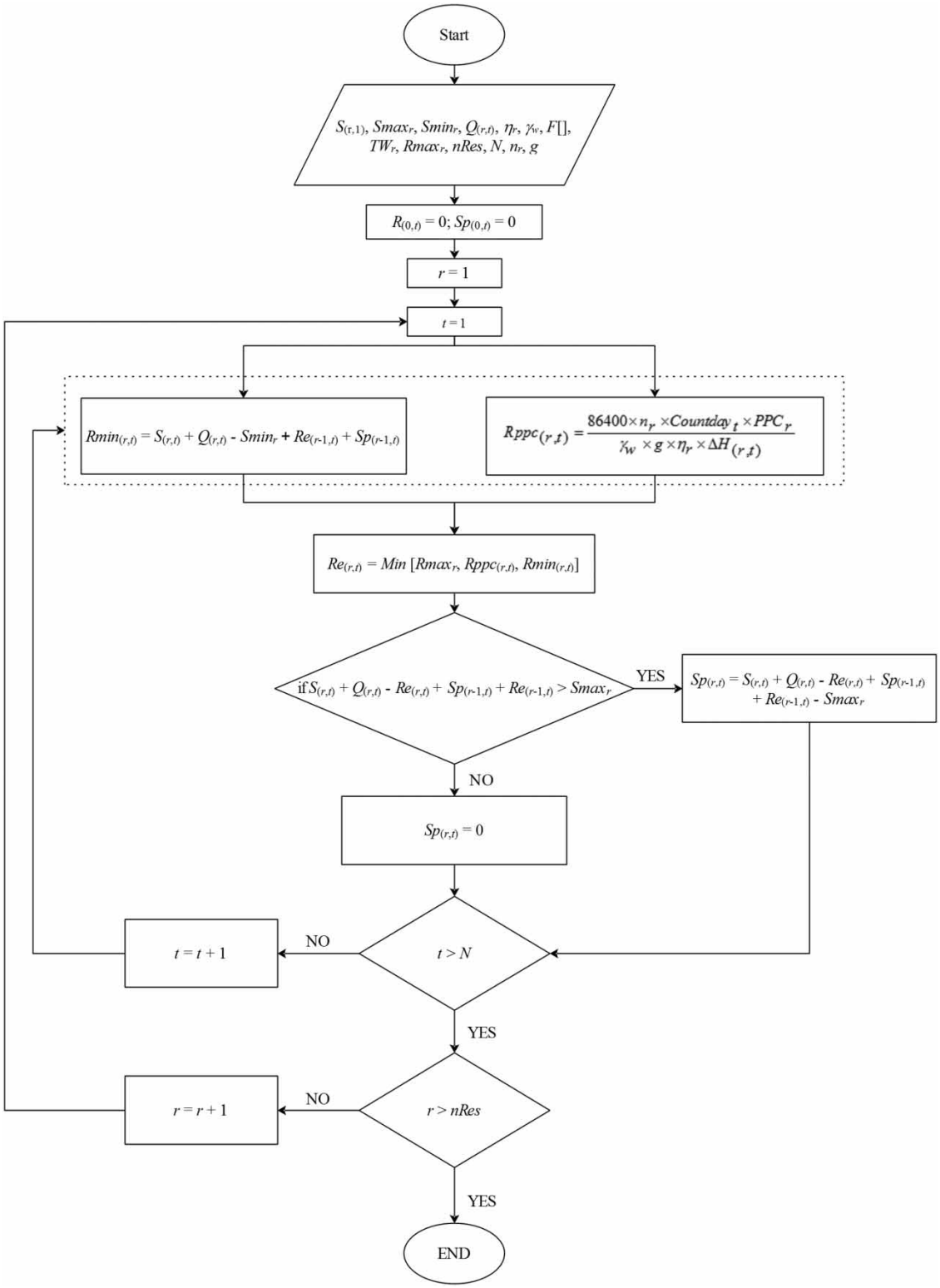

Figure 3 | Flowchart of the hydropower system SOP (*Notes:* PPC_r = hydropower plant capacity of the rth reservoir; $Rppc_{(r,t)}$ = maximum volume of water that can be withdrawn from the rth reservoir at the tth time step without violating the introduced constraint in Equation (13); and $Rmin_{(r,t)}$ = maximum volume of water that can be withdrawn from the rth reservoir at the tth time step without violating the introduced constraint in Equation (14)).

in which α_r = reliability of the rth reservoir's hydropower system. Reliability has a range of [0,1].

The resiliency criterion of a hydropower system, which is defined as the conditional probability of a successful state event given that a failure event has occurred, can be defined as:

$$\gamma_r = \frac{\sum_{t=1}^{N-1} W_{(r,t)}}{N - \sum_{t=1}^{N} W_{(r,t)}} \quad r = 1, \ldots, n\text{Res} \tag{21}$$

in which, γ_r = resiliency of the rth reservoir's hydropower system; and $W_{(r,t)}$ is given by:

$$W_{(r,t)} = \begin{cases} 1 & if \quad X_{(r,t+1)} = 1 \& X_{(r,t)} = 0 \\ 0 & else \end{cases} \quad r = 1, \ldots, nRes; t = 1, \ldots, N \tag{22}$$

Note that resiliency has a range of [0,1].

Unlike reliability and resiliency, vulnerability does not have a unique definition. While many interpretations of vulnerability are effective in system assessments, they are also subject to certain drawbacks (Zolghadr-Asli *et al.* 2016b). In order to overcome these drawbacks, the vulnerability of a hydropower system can be redefined as:

$$\upsilon_r = \frac{\sum_{X_{(r,t)} \in F} f_{(r,t)} \times e_{(r,t)}}{PPC_r} \quad r = 1, \ldots, n\text{Res} \tag{23}$$

$$f_{(r,t)} = PPC_r - PP_{(r,t)} \quad r = 1, \ldots, n\text{Res}; t = 1, \ldots, N \tag{24}$$

in which, υ_r = vulnerability of the rth reservoir's hydropower system; $f_{(r,t)}$ = severity of each probable failure for the rth reservoir's hydropower system at the tth time step; and $e_{(r,t)}$ = a weight specified for each probable failure in the rth reservoir's hydropower system at the tth time step, which is given by:

$$e_{(r,t)} = \frac{f_{(r,t)}}{\sum_{X_{(r,t)} \in F} f_{(r,t)}} \quad r = 1, \ldots, n\text{Res}; t = 1, \ldots, N \tag{25}$$

Consequently, the vulnerability of a hydropower system can be rewritten as:

$$\upsilon_r = \frac{\sum_{X_{(r,t)} \in F} ([f_{(r,t)}]^2 / \sum_{X_{(r,t)} \in F} f_{(r,t)})}{PPC_r} \quad r = 1, \ldots, n\text{Res} \tag{26}$$

Note that, as far as the operation and performance analyses of such a hydropower system are concerned, the proposed definition of vulnerability (Equation (26)) is considered as a novel attempt, and, as stated earlier, given the conceptual advantages of the proposed formulation of vulnerability, a more accurate evaluation of the hydropower system can be expected by employing the aforementioned proposition for the vulnerability criterion.

The PBPC and RRV have been proven to be effective for evaluating water resources systems. The flexibility, along with other merits such as avoidance of unnecessary computational complexity, makes them a logical first choice for water resources systems analysis (Butler *et al.* 2014). While the preliminary application of the aforementioned criteria is to quantify the performance of any system, given the probabilistic nature of these criteria, RRV can also be used to analyze the uncertainties that are associated with complex systems. Although a few have attempted to employ these criteria to deal with uncertain conditions of water resources (e.g. Fowler *et al.* 2003; Ashofteh *et al.* 2016; Mateus & Tullos 2016), to the best of our knowledge, no comprehensive yet easily computable framework has been developed based upon the RRV criteria in order to analyze the uncertainties of complex hydropower systems.

STUDY AREA

As stated earlier, many developing nations neglect to assess the potential impacts of climate change on the performance of hydropower systems. In Iran, the second largest country in the Middle East, for instance, hydropower production plays a crucial role in supplying the peak power demand. While hydropower accounts for approximately 11% of the nation's electricity and is thus, by far, the largest renewable energy source, such assessments have minimal impact on the design phase of hydropower systems. Considering the boom in global hydropower (Zarfl *et al.* 2015), Iran is also actively attempting to expand its hydropower systems. Currently, most of Iran's hydroelectric plants are concentrated in three major river basins: the Karun, Dez, and Karkheh River basins. The Karkheh River basin can be listed as one of the three most productive basins in Iran in terms of total surface water flow and subsequently the potential for

hydropower generation. Consequently, Iranian authorities actively pursue the expansion of the Karkheh River basin's capacity for hydroelectricity generation. Given the value of hydropower and its current development state in the Middle East, in this study the Karkheh River basin was selected as an example to demonstrate the proposed framework. Additionally, such studies also underline the value of proactive assessment of the impacts of climate change on the performance of hydropower systems. It should be noted that such studies are considered as the bedrocks on which further milestone, in-depth risk assessment studies ought to be based, since evaluating the extremes in a risk analysis for design or planning of water resources systems requires further investigations and finer spatial and temporal scales.

The Karkheh River originates from the Zagros Mountains in west Iran. After a journey of approximately 900 km, the Karkheh River discharges into the Hoor-Al-Azim swamp at the Iran–Iraq border. The Karkheh River basin, with a catchment area of 51,000 km^2, is located in the south-western region of Iran (latitude: 30–35° N; longitude: 46–49° E). The elevation of the Karkheh basin varies from a few meters above sea level (m.a.s.l.), mostly in the southern part of the basin, to more than 3,500 m.a.s.l. in the northeast part of the basin. Dominated by the Mediterranean climate, more than 64% of the annual water flow occurs from January to May.

The basin experiences high spatio-temporal variations in rainfall and air temperature (Muthuwatta *et al.* 2010). The southern part of the basin receives an average annual rainfall of approximately 150 mm, while in the northern and northeast parts of the basin, it is as high as 1,000 mm. The air temperature in this area, however, ranges from −25 to 50 °C. Thus, the southern area of the catchment can be classified as semi-arid with mild winters and long hot summers, while the northern parts and the alpine regions have cold winters and mild summers. Figures 4 and 5, respectively, show the average monthly rainfall and air temperature data at four climate stations in the basin. Based on the elevations and relative locations in the basin, all stations are grouped into north, center, and south (Table 1).

The average annual discharge of the Karkheh River is 5,916 million m^3 (MCM). Major water consumers in the basin include agricultural, municipal, and fish farming

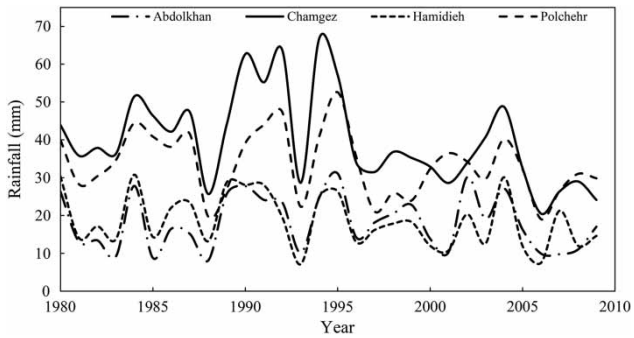

Figure 4 | Average monthly rainfall in the baseline period (1980–2009).

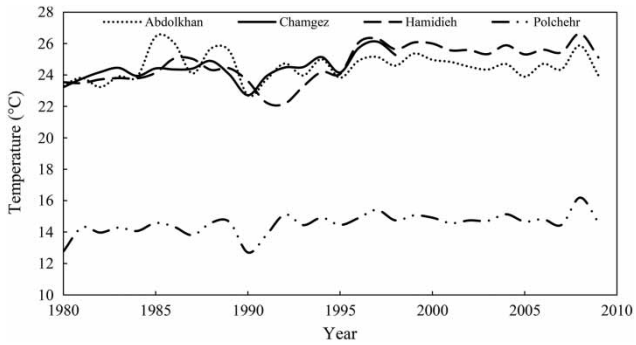

Figure 5 | Average monthly air temperature in the baseline period (1980–2009).

Table 1 | Climate stations in the study area

Station	Elevation (m.a.s.l.)	Latitude (N)	Longitude (E)	Location
Polchehr	1,275	34° 20′	47° 26′	North
Chamgez	380	32° 56′	47° 50′	Center
Abdolkhan	40	31° 50′	48° 23′	South
Hamidieh	20	31° 29′	48° 26′	

m.a.s.l., meters above sea level.

users (Jamali *et al.* 2013). In the northern parts of the basin, both rainfed and irrigated agricultural practices are adopted. In the drier southern regions of the basin, however, irrigated agriculture is the dominant practice. In order to enhance the accuracy of hydrologic simulation, the Karkheh River basin is divided into two major parts: the upstream river (namely Seimareh River) and the downstream river (Karkheh River) (Figure 6), and separate model calibration is performed for each part.

Given the great potential of the Karkheh River basin for hydroelectric generation, many hydropower projects are

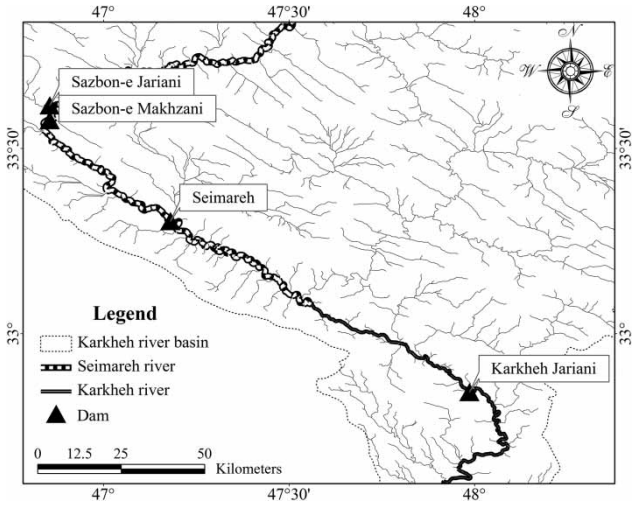

Figure 6 | Locations of the study area and hydropower plants.

under consideration, one of which has already been constructed, and the procedure to bring it to an operational state has begun. Four dams selected for this study are exclusively used for hydropower generation purposes and are either under study or have just began their operation. The characteristics of these dams and their locations are shown in Table 2 and Figure 6, respectively.

Table 2 | Descriptions of hydropower projects in the study area

	Dam			
	Sazbon-e Jariani	**Sazbon-e Makhzani**	**Seimareh**	**Karkheh Jariani**
Normal water table (m.a.s.l.)	875	850	720	375
Inactive water table (m.a.s.l.)	865	830	705	370
Normal storage (MCM)	516	1,576	2,474	132
Inactive storage (MCM)	398	918	1,664	92
Installation capacity (MW)	366	300	480	360
Plant factor	0.16	0.16	0.16	0.25
Power plant efficiency	0.935	0.930	0.935	0.930
Current condition	Under study	Under study	Completed	Under study

m.a.s.l., meters above sea level; MCM, million cubic meter; MW, megawatt.

RESULTS AND DISCUSSION

Constructed climate change scenarios

This study used the CanESM2 model to simulate rainfall and air temperature for the RCP 2.6, RCP 4.5, and RCP 8.5 scenarios. The baseline period ranged from 1980 to 2009, while the climate change period included 90 years from 2010 to 2099. Using the change factor technique and SDSM, the results from the CanESM2 model were then downscaled. Brief summaries of the constructed climate scenarios using the change factor technique and SDSM are shown in Tables 3 and 4, respectively.

The results of the change factor technique indicated that, while the basin's average air temperature rose in all the scenarios, the patterns of rainfall could vary in each constructed scenario. For instance, the change factor technique predicted an increase of 0.5, 0.6, and 0.8 °C in the average air temperature for RCP 2.6, RCP 4.5, and RCP 8.5, respectively. As shown in Table 4, the results of the SDSM show increases in both rainfall and air temperature. Also, these predicted changes are more extreme than those from the change factor techniques. According to Table 4, for instance, an increase of 0.7, 0.8, and 1.1 °C in the average air temperature could be expected for RCP 2.6, RCP 4.5, and RCP 8.5, respectively.

A comparison of the results from the change factor technique and SDSM confirms the fact that SDSM could provide a better prediction, especially for extreme climate conditions. The changes in the frequency of climate patterns are seldom consistent with those produced by the host GCM, except for the cases in which additional predictors (e.g. atmospheric humidity) are employed (Wilby & Dawson 2007). As a result, the change factor technique would generate milder changes, while SDSM could predict stronger changes.

After construction of the climate scenarios, the basin's hydrologic responses to such upcoming events were then simulated using the IHACRES model. Additionally, the model was calibrated separately for the basin's main upstream river (Seimareh River) and downstream river (Karkheh River). The quantitative statistical parameters for evaluating the calibration and validation results are listed

Table 3 | Differences between the climate change conditions predicted by the change factor technique for 2010–2039, 2040–2069, and 2070–2099 and the baseline condition (1980–2009)

			(2010–2039)			(2040–2069)			(2070–2099)		
		Year Location	Min.	Average	Max.	Min.	Average	Max.	Min.	Average	Max.
RCP 2.6	Rainfall (mm)	North	−5.2	−0.2	5.4	−3.3	1.1	7.6	0.2	0.4	0.5
		Center	−8.1	−0.5	6.9	−5.1	1.0	9.5	−7.1	0.4	6.8
		South	−10.9	−0.4	6.6	−6.9	0.7	6.5	−9.3	−0.1	4.0
	Air temperature (°C)	North	0.1	0.4	0.9	0.2	0.4	0.8	0.2	0.4	0.9
		Center	–	–	–	–	–	–	–	–	–
		South	0.1	0.5	1.3	0.2	0.6	1.5	0.2	0.6	1.6
RCP 4.5	Rainfall (mm)	North	−4.1	0.3	4.9	−6.4	−0.3	7.2	−6.3	−0.2	4.3
		Center	−4.5	0.1	4.6	−7.4	−0.7	7.3	−5.9	−0.4	4.9
		South	−9.8	0.0	4.4	−10.5	−0.2	6.1	−11.4	−0.2	4.2
	Air temperature (°C)	North	0.1	0.3	0.6	0.1	0.5	1.1	0.2	0.6	1.3
		Center	–	–	–	–	–	–	–	–	–
		South	0.2	0.5	1.1	0.2	0.7	1.6	0.3	0.9	2.0
RCP 8.5	Rainfall (mm)	North	−4.1	0.4	10.0	−8.1	0.8	11.2	−9.2	0.7	8.4
		Center	−6.3	0.0	4.6	−4.9	1.4	14.2	−6.4	0.7	7.4
		South	−10.2	0.3	6.9	−6.0	0.9	12.6	−3.2	1.1	7.0
	Air temperature (°C)	North	0.1	0.3	0.8	0.2	0.6	1.3	0.4	0.9	1.8
		Center	–	–	–	–	–	–	–	–	–
		South	0.2	0.5	1.2	0.3	0.9	2.1	0.5	1.3	2.9

Table 4 | Differences between the climate change conditions predicted by SDSM for 2010–2039, 2040–2069, and 2070–2099 and the baseline condition (1980–2009)

			(2010–2039)			(2040–2069)			(2070–2099)		
		Year Location	Min.	Average	Max.	Min.	Average	Max.	Min.	Average	Max.
RCP 2.6	Rainfall (mm)	North	−9.3	3.2	22.3	−7.8	2.8	22.6	−5.0	3.6	21.7
		Center	–	–	–	–	–	–	–	–	–
		South	−7.5	1.1	27.0	−7.8	1.4	26.8	−13.6	1.3	25.1
	Air temperature (°C)	North	–	–	–	–	–	–	–	–	–
		Center	−0.7	0.2	0.7	−0.4	0.3	1.1	−1.0	0.3	1.1
		South	−0.1	1.1	2.7	0.0	1.2	2.7	0.1	1.2	2.8
RCP 4.5	Rainfall (mm)	North	−6.8	4.1	24.5	−7.2	3.7	20.2	−6.7	3.2	17.2
		Center	–	–	–	–	–	–	–	–	–
		South	−12.6	0.8	25.6	−8.2	0.6	25.1	−9.9	1.0	24.8
	Air temperature (°C)	North	–	–	–	–	–	–	–	–	–
		Center	−1.2	0.0	0.8	−0.3	0.4	1.3	0.1	0.7	1.8
		South	−0.1	1.1	2.4	0.0	1.3	2.7	0.0	1.4	3.0
RCP 8.5	Rainfall (mm)	North	−3.9	3.5	18.2	−6.6	3.2	17.7	−13.5	4.3	27.3
		Center	–	–	–	–	–	–	–	–	–
		South	−9.6	1.6	27.8	−13.3	0.3	25.0	−11.5	0.9	22.7
	Air temperature (°C)	North	–	–	–	–	–	–	–	–	–
		Center	−1.3	0.1	0.7	−0.4	0.6	1.7	0.4	1.4	3.5
		South	0.0	1.1	2.6	0.0	1.5	3.2	0.0	1.9	4.5

in Table 5. The observed and simulated streamflows of the Seimareh River and Karkheh River are illustrated in Figures 7 and 8, respectively. As shown in Table 5, all indicators are in the acceptable ranges. Table 6 summarizes the predicted flows of both rivers (Seimareh River and Karkheh River) for the constructed climate scenarios. The

Table 5 | Quantitative evaluations of model calibration and validation results for Seimareh River and Karkheh River

Seimareh River	Calibration	*NSE*	0.75
		PB	4.46
		RSR	0.50
	Validation	*NSE*	0.60
		PB	1.18
		RSR	0.63
Karkheh River	Calibration	*NSE*	0.58
		PB	11.48
		RSR	0.65
	Validation	*NSE*	0.67
		PB	−18.88
		RSR	0.57

NSE, Nash–Sutcliffe model efficiency coefficient; *PB*, percent bias; and *RSR*, ratio of root-mean-square error.

results indicated that mostly SDSM predicted higher values for average and minimum streamflow, while the change factor technique predicted higher values for maximum streamflow.

Finally, in order to quantify the impacts of climate change on hydropower systems, and analyze the uncertainties that are associated with such assessments, the hydropower system SOP (Figure 3) was applied to the four-reservoir hydropower system for both baseline and climate change conditions. Figures 9 and 10 respectively show the box plots of the system's total hydropower generation under the assumptions of RCP 2.6, using the results downscaled by the change factor technique and SDSM. Additionally, as an example, Table 7 summarizes the central tendency (mode, median, and average) and disperse indicators (range, standard deviation, and skewness) for January under both baseline and climate change conditions.

For the central tendency in January, the mode of the total hydropower generated by the system for both baseline and climate change conditions is 1,506 MW. In fact, this would also be the case for all other months, except August, September, and October. Knowing that this value is also the capacity of the hydropower system could be a sign of a well-designed system. Additionally, comparison of the median of the hydroelectricity generated for the baseline condition (1,433 MW) and the climate change conditions revealed that in at least half of the time in January the results produced by the change factor technique had a lower median, while SDSM yielded hydroelectricity production with a higher median than that for the baseline condition. This would also be the case in February, June, August, September, October, November, and December. In March, April, and May, the same median was obtained for the baseline and climate change conditions. In July, the median under both climate change conditions was higher than

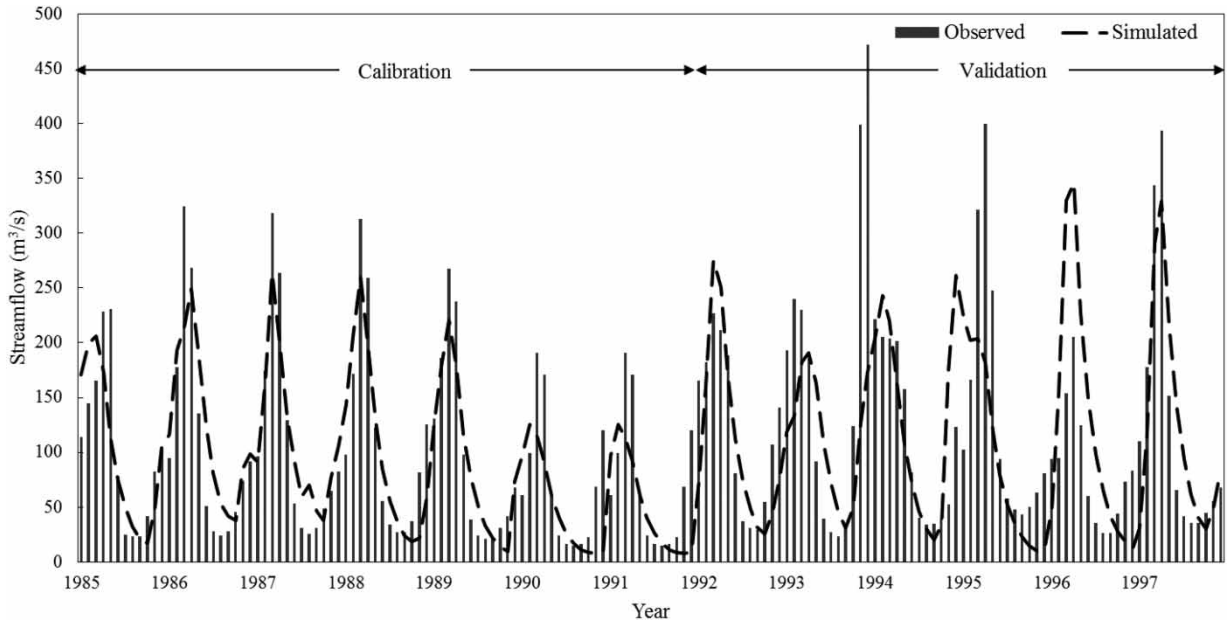

Figure 7 | Simulated and observed streamflow of Seimareh River.

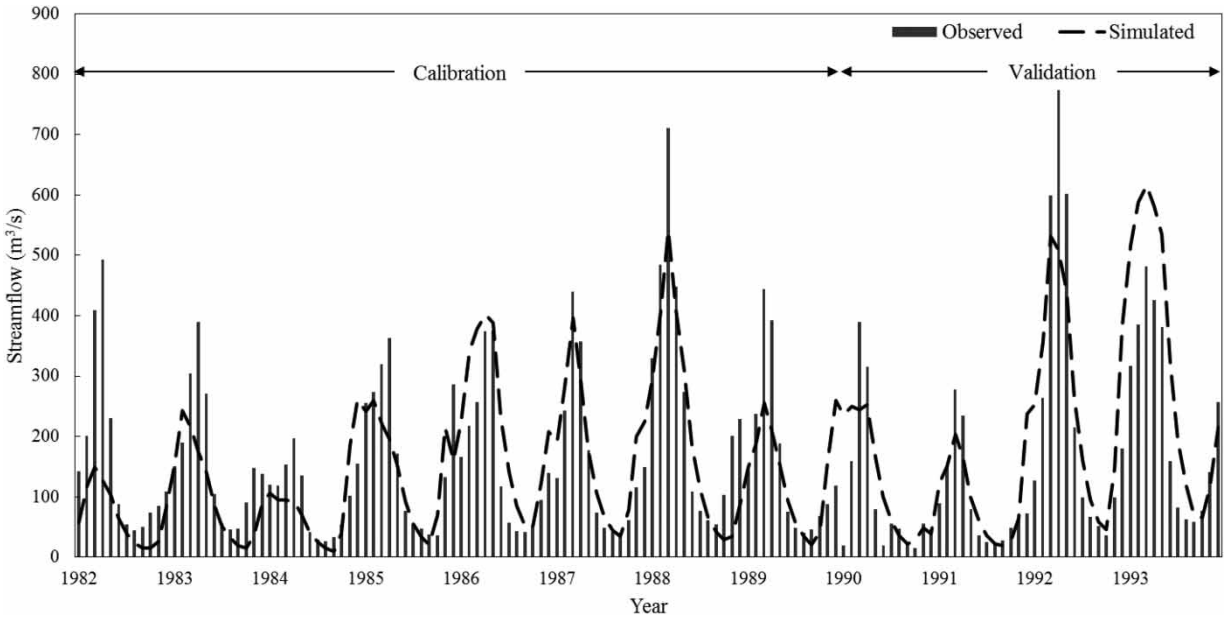

Figure 8 | Simulated and observed streamflow of Karkheh river.

Table 6 | Discharges (m^3/s) of Seimareh River and Karkheh River under climate change conditions

			(2010–2039) Discharge (m^3/s)			(2040–2069)			(2070–2099)		
		Year River	Min.	Average	Max.	Min.	Average	Max.	Min.	Average	Max.
RCP 2.6	Change factor	Seimareh	2	73	312	2	78	331	2	77	319
		Karkheh	6	142	844	6	156	909	6	151	855
	SDSM	Seimareh	10	101	283	15	101	281	14	105	289
		Karkheh	7	156	496	25	171	469	24	171	432
RCP 4.5	Change factor	Seimareh	2	74	319	2	73	305	2	74	321
		Karkheh	6	146	883	5	142	814	6	143	831
	SDSM	Seimareh	9	107	271	13	106	348	16	101	297
		Karkheh	8	152	439	23	166	430	28	171	491
RCP 8.5	Change factor	Seimareh	2	75	332	2	80	338	2	79	340
		Karkheh	6	146	893	6	156	849	6	148	819
	SDSM	Seimareh	6	103	276	14	102	329	14	104	318
		Karkheh	5	169	514	21	144	426	19	147	424

SDSM, statistical downscaling model.

that for the baseline condition. Another way to analyze the central tendency of the hydropower generations is to use the average of the data. For instance, a comparison between the average values for the baseline and climate change conditions revealed that the system showed a better performance under the baseline condition than the condition of climate changes projected by the change factor technique. However, the condition and performance of the system were improved for the SDSM results. In fact, this was the case for the rest of the months.

In addition, to gain a comprehensive overview of the generated results, the disperse indicators were also analyzed. The results indicated that in January the range of the generated results for the baseline condition was more

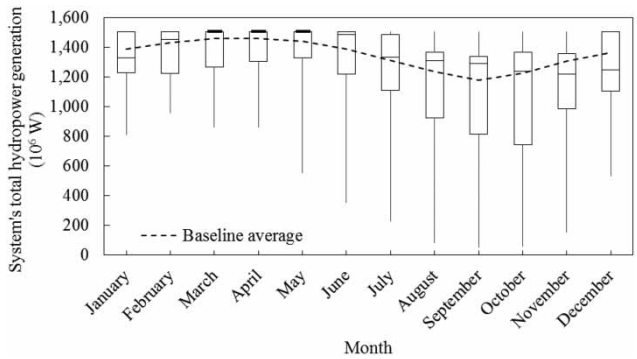

Figure 9 | Box plot of monthly hydropower of the system predicted by the change factor technique for the climate change condition.

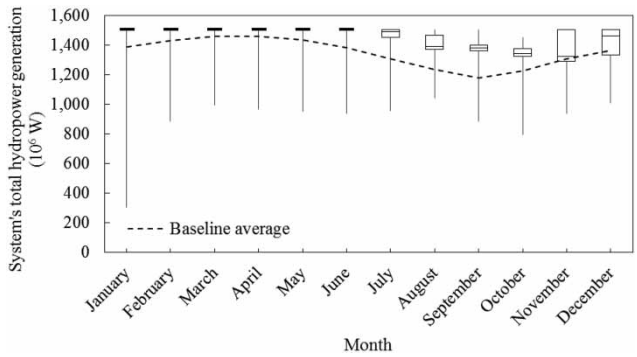

Figure 10 | Box plot of monthly hydropower of the system predicted by SDSM for the climate change condition.

than that for the climate change conditions. SDSM resulted in a higher range than the change factor technique for January. However, this was not the case for other months, in which the smallest range was obtained for the baseline condition compared to the climate change conditions, and in most cases, SDSM provided a lower range than the change factor technique. Additionally, analyzing the standard division showed that in January the standard deviation for the baseline condition was higher than that for the climate change conditions. The change factor technique yielded a higher standard deviation than SDSM in January, although this was not the case for other months, in which the SDSM results demonstrated a lower standard deviation compared to the baseline condition, while the results of the change factor technique yielded an even lower standard deviation in comparison. Finally, analyzing skewness revealed that the results for all the simulated conditions (both baseline and climate change conditions) exhibited left-tails, indicating that the generated data were unevenly distributed, which could also be observed from comparison of the median and the average of the data for each condition (median > average). This reflects low-frequency data, with a low total hydropower generation. In most months, the highest absolute values of the skewness were observed, in order, in the results from SDSM for the baseline condition, and from the change factor technique.

Although such analyses can provide a primary insight into the uncertainties associated with the generated hydropower electricity, given the massive created database, a comprehensive oversight of the performance of a system is a technical, time-consuming process. While using the RRV may not ease the analysis process, it could pinpoint the potential risk of the system's performance, and how it could affect the system, which in fact is the initial step to manage such plausible hazards. These analyses provide the probability of a failure event (reliability, Figure 11), the likelihood of achieving an acceptable performance if a failure would have occurred (resiliency, Figure 12), and the severity of these probable failures (vulnerability, Figure 13), as well as summarizing

Table 7 | Central tendency and disperse indicators of generated hydroelectricity under baseline and climate change conditions

			Central tendency			Disperse indicators		
			Mode (MW)	Median (MW)	Average (MW)	Range (MW)	Standard deviation (MW)	Skewness
Baseline			1,506	1,433	1,390	1,309	125	−0.60
Climate change	Change factor	RCP 2.6	1,506	1,328	1,315	698	191	−0.75
		RCP 4.5	1,506	1,313	1,302	656	199	−0.65
		RCP 8.5	1,506	1,356	1,339	647	177	−0.84
	SDSM	RCP 2.6	1,506	1,506	1,479	1,203	139	−7.23
		RCP 4.5	1,506	1,506	1,485	1,165	131	−7.83
		RCP 8.5	1,506	1,506	1,483	1,144	128	−7.81

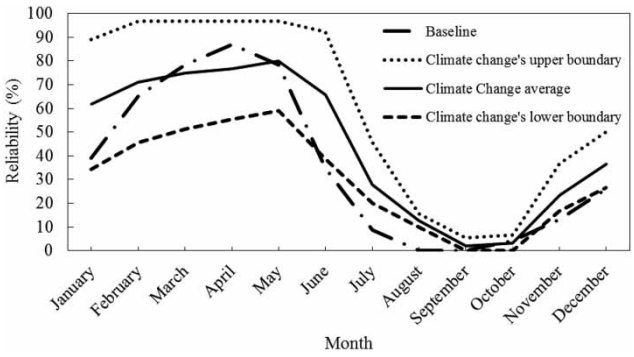

Figure 11 | Reliability of the hydropower system under the baseline and climate change condition.

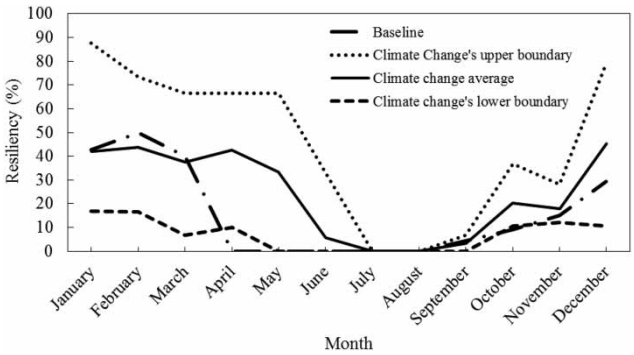

Figure 12 | Resiliency of the hydropower system under the baseline and climate change condition.

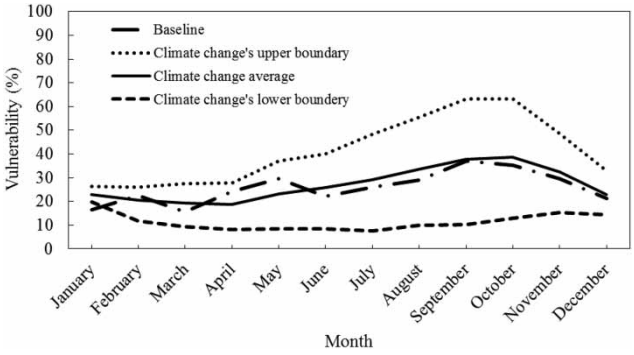

Figure 13 | Vulnerability of the hydropower system under the baseline and climate change condition.

the performance of a system in terms of these three probability-based criteria.

It was found from analyzing the performance of the hydropower system that considering the reliability, resiliency, and vulnerability criteria, the best performances in the climate change condition occurred in May (80% reliability), December (45% resiliency), and April (19% vulnerability). Yet the worst performances occurred in September (2% reliability), July and August (0% resiliency), and October (39% vulnerability). It should be noted that the aforementioned analysis of the performances of the hydropower system was based on the average projections for the climate change condition. Given the uncertainties embedded in the climate construction procedure, the represented values may not be the only trajectories for future conditions. For instance, analyzing the range of the performance criteria for each month (the difference between upper and lower boundaries in each month) could account for the uncertainty in the predicted results. The larger the range is, the more uncertain the predictions can be. For instance, January, with a range of 54% in predicting the reliability of the hydropower system, has the highest uncertainty, while the represented value decreases to 6% in September and October. Naturally, this indicates that there is less certainty in the reliability predicted for January than the reliability of the system predicted for September and October, per se. The analysis also indicates that considering the resiliency criterion, January (71%) has the highest uncertainty in the predicted resiliency, while both July and August (0%) have almost no uncertainty in their predicted resiliency. Considering the vulnerability criterion, September (53%) and January (7%) respectively have the lowest and highest ranges.

A comparison of the results for the baseline and climate change condition revealed that, except for the decrements in March (3%), April (10%), and October (1%), in other months the chances of successful performance of the system in the climate change condition increased (reliability). Analyzing the resiliency in both baseline and climate change condition also indicated that the system performance would be improved under the climate change condition. Nevertheless, unlike the aforementioned criteria, the vulnerability of the system increased (worsened) for most months, except for the decrements in February (2%) and May (6%). It can be concluded from such changing patterns that although the system was more likely to show an acceptable performance, and in the case of a failure the system was more likely to change to a better situation, yet the probable failures were more severe and may have caused more harm due to the upcoming climate conditions. Consequently, such results indicate that a backup system may be required to help support the system in the case of a failure.

CONCLUDING REMARKS

This study was aimed at assessing the potential impacts of climate change on hydropower system performance and the uncertainties associated with such assessments. To do so, the CanESM2 model, and RCP 2.6, RCP 4.5, and RCP 8.5 were used to generate large-scale climate change scenarios in the Karkheh River basin, Iran. The results were then downscaled by using the change factor technique and SDSM. While both approaches demonstrated increases in the air temperatures simulated for the climate change conditions, different rainfall patterns were predicted. While the results from the change factor technique indicated milder climate changes in the region, SDSM predicted severe climate changes. Additionally, the SDSM predictions showed a slight improvement in the region's water resources conditions, while the change factor technique predicted a mild downturn instead. Such results underlined the importance of the downscaling techniques. To evaluate the impacts of climate change on the hydropower system, their performance criteria (reliability, resiliency, and vulnerability) were used to assess and quantify the uncertainties that were associated with such assessments. These results indicated that both reliability and resiliency of the hydropower system were improved due to climate changes, while the vulnerability of the system would increase (worsen). This suggests that, although the system might not fail frequently, severe blackouts might occur. With timely consideration of future climatic conditions and appropriate adaptive actions, including additional backup systems for reliable and safe electricity generation, future undesired conditions can be avoided in the basin. Note that this study exclusively investigated the uncertainties that are rooted in the related climate change scenarios. Hence, for further investigations, other sources of climate change uncertainties (e.g. GCM models) can also be explored.

REFERENCES

Abushandi, E. & Merkel, B. 2013 Modelling rainfall runoff relations using HEC-HMS and IHACRES for a single rain event in an arid region of Jordan. *Water Resour. Manage.* **27** (7), 2391–2409.

Adhikari, U., Nejadhashemi, A. P., Herman, M. R. & Messina, J. P. 2016 Multiscale assessment of the impacts of climate change on water resources in Tanzania. *J. Hydrol. Eng.* **22** (2), 05016034.

Ashofteh, P.-S., Bozorg-Haddad, O. & Loáiciga, H. A. 2016 Role of adaptive water resources management policies and strategies in relieving conflicts between water resources and agricultural sector water use caused by climate change. *J. Irrig. Drain. Eng.* **143** (5), 02516004.

Bergström, S., Carlsson, B., Gardelin, M., Lindström, G., Pettersson, A. & Rummukainen, M. 2001 Climate change impacts on runoff in Sweden assessments by global climate models, dynamical downscaling and hydrological modelling. *Clim. Res.* **16** (2), 101–112.

Butler, D., Farmani, R., Fu, G., Ward, S., Diao, K. & Astaraie Imani, M. 2014 A new approach to urban water management: Safe and sure. In: *16th Conference on Water Distribution System Analysis (WDSA)*, Bari, Italy, 14–17 July.

Chandel, S. S., Shrivastva, R., Sharma, V. & Ramasamy, P. 2016 Overview of the initiatives in renewable energy sector under the national action plan on climate change in India. *Renew. Sustain. Energy Rev.* **54**, 866–873.

Chen, X. Y., Chau, K. W. & Busari, A. O. 2015 A comparative study of population-based optimization algorithms for downstream river flow forecasting by a hybrid neural network model. *Eng. Appl. Artif. Intell.* **46**, 258–268.

Chylek, P., Li, J., Dubey, M. K., Wang, M. & Lesins, G. 2011a Observed and model simulated 20th century Arctic temperature variability: Canadian earth system model CanESM2. *Atmos. Chem. Phys. Discuss.* **11** (8), 22893–22907.

Chylek, P., Folland, C. K., Dijkstra, H. A., Lesins, G. & Dubey, M. K. 2011b Ice-core data evidence for a prominent near 20 year time-scale of the Atlantic Multidecadal Oscillation. *Geophys. Res. Lett.* **38** (13), L13704.

Christensen, N. S., Wood, A. W., Voisin, N., Lettenmaier, D. P. & Palmer, R. N. 2004 The effects of climate change on the hydrology and water resources of the Colorado River basin. *Climatic Change* **62** (1–3), 337–363.

Collins, M. & Allen, M. R. 2002 Assessing the relative roles of initial and boundary conditions in interannual to decadal climate predictability. *J. Clim.* **15** (21), 3104–3109.

Connell-Buck, C. R., Medellín-Azuara, J., Lund, J. R. & Madani, K. 2011 Adapting California's water system to warm vs. dry climates. *Clim. Change* **109** (1), 133–149.

Dijkstra, H. A., Te Raa, L., Schmeits, M. & Gerrits, J. 2006 On the physics of the Atlantic multidecadal oscillation. *Ocean Dynam.* **56** (1), 36–50.

Dincer, I. & Acar, C. 2015 A review on clean energy solutions for better sustainability. *Int. J. Energy Res.* **39** (5), 585–606.

Dye, P. J. & Croke, B. F. 2003 Evaluation of streamflow predictions by the IHACRES rainfall-runoff model in two South African catchments. *Environ. Model. Softw.* **18** (8), 705–712.

El-Baroudy, I. & Simonovic, S. P. 2004 Fuzzy criteria for the evaluation of water resources systems performance. *Water Resour. Res.* **40** (10), W10503.

Ermini, E. & Ataoui, R. 2013 Computing a global performance index by fuzzy set approach. In: *12th International Conference on Computing and Control for Water Industry (CCWI2013)*, Perugia, Italy, 2–4 September.

Fiering, M. B. 1982 Alternative indices of resilience. *Water Resour. Res.* **18** (1), 33–39.

Fowler, H. J., Kilsby, C. G. & O'Connell, P. E. 2003 Modeling the impacts of climatic change and variability on the reliability, resilience, and vulnerability of a water resource system. *Water Resour. Res.* **39** (8), 1–10.

Guégan, M., Uvo, C. B. & Madani, K. 2012 Developing a module for estimating climate warming effects on hydropower pricing in California. *Energy Pol.* **42**, 261–271.

Gupta, H. V., Sorooshian, S. & Yapo, P. O. 1999 Status of automatic calibration for hydrologic models: comparison with multilevel expert calibration. *J. Hydrol. Eng.* **4** (2), 135–143.

Halbouty, M. T. 1990 *Giant Oil and Gas Fields of the Decade.* The American Association of Petroleum Geologists, Tulsa, Oklahoma.

Hansen, D. P., Ye, W., Jakeman, A. J., Cooke, R. & Sharma, P. 1996 Analysis of the effect of rainfall and streamflow data quality and catchment dynamics on streamflow prediction using the rainfall-runoff model IHACRES. *Environ. Softw.* **11** (1), 193–202.

Hashimoto, T., Loucks, D. P. & Stedinger, J. R. 1982a Robustness of water resources systems. *Water Resour. Res.* **18** (1), 21–26.

Hashimoto, T., Stedinger, J. R. & Loucks, D. P. 1982b Reliability, resiliency, and vulnerability criteria for water resource system performance evaluation. *Water Resour. Res.* **18** (1), 14–20.

Hashmi, M. Z., Shamseldin, A. Y. & Melville, B. W. 2011 Comparison of SDSM and LARS-WG for simulation and downscaling of extreme precipitation events in a watershed. *Stoch. Environ. Res. Risk Assess.* **25** (4), 475–484.

International Energy Agency (IEA) 2016 *The Key World Energy Statistics.* Head of Communication and Information Office, Paris, France.

IPCC 2007 *Climate Change 2007: The Physical Science Basis*. Contribution of Working Group I to the Fourth Assessment Report of the Intergovernmental Panel on Climate Change, Cambridge University Press, Cambridge, NY.

IPCC 2013 *Climate Change 2013: The Physical Science Basis*. Contribution of Working Group I to the Fifth Assessment Report of the Intergovernmental Panel on Climate Change, Cambridge University Press, Cambridge, NY.

IPCC 2014a *Climate Change 2014: Impacts, Adaptation, and Vulnerability*. Contribution of Working Group II to the Fifth Assessment Report of the Intergovernmental Panel on Climate Change, Cambridge University Press, Cambridge, NY.

IPCC 2014b *Climate Change 2014: Mitigation of Climate Change*. Contribution of Working Group III to the Fifth Assessment Report of the Intergovernmental Panel on Climate Change, Cambridge University Press, Cambridge, NY.

Jakeman, A. J. & Hornberger, G. M. 1993 How much complexity is warranted in a rainfall-runoff model? *Water Resour. Res.* **29** (8), 2637–2649.

Jamali, S., Abrishamchi, A. & Madani, K. 2013 Climate change and hydropower planning in the Middle East: implications for Iran's Karkheh hydropower systems. *J. Energy Eng.* **139** (3), 153–160.

Kundzewicz, Z. W. & Laski, A. 1995 *New Uncertainties Concepts in Hydrology and Water Resources.* Cambridge University Press, Cambridge, USA.

Liu, X., Tang, Q., Voisin, N. & Cui, H. 2016 Projected impacts of climate change on hydropower potential in China. *Hydrol. Earth Syst. Sci.* **20** (8), 3343–3359.

Mateus, M. C. & Tullos, D. 2016 Reliability, sensitivity, and vulnerability of reservoir operations under climate change. *J. Water Resour. Plan. Manage.* **143** (4), 04016085.

Meenu, R., Rehana, S. & Mujumdar, P. P. 2013 Assessment of hydrologic impacts of climate change in Tunga–Bhadra river basin, India with HEC-HMS and SDSM. *Hydrol. Process.* **27** (11), 1572–1589.

Medellín-Azuara, J., Harou, J. J., Olivares, M. A., Madani, K., Lund, J. R., Howitt, R. E., Tanaka, S. K., Jenkins, M. W. & Zhu, T. 2008 Adaptability and adaptations of California's water supply system to dry climate warming. *Clim. Change* **87**, 75–90.

Meyer, E. S., Characklis, G. W. & Brown, C. 2017 Evaluating financial risk management strategies under climate change for hydropower producers on the Great Lakes. *Water Resour. Res.* **53** (3), 2114–2132.

Minville, M., Brissette, F., Krau, S. & Leconte, R. 2009 Adaptation to climate change in the management of a Canadian water-resources system exploited for hydropower. *Water Resour. Manage.* **23** (14), 2965–2986.

Minville, M., Krau, S., Brissette, F. & Leconte, R. 2010 Behaviour and performance of a water resource system in Québec (Canada) under adapted operating policies in a climate change context. *Water Resour. Manage.* **24** (7), 1333–1352.

Mishchenko, M. I., Liu, L., Geogdzhayev, I. V., Travis, L. D., Cairns, B. & Lacis, A. A. 2010 Toward unified satellite climatology of Aerosol properties: MODIS versus MISR versus AERONET. *J. Quant. Spectrosc. Radiat. Transf.* **111** (4), 540–552.

Moriasi, D. N., Arnold, J. G., Van Liew, M. W., Bingner, R. L., Harmel, R. D. & Veith, T. L. 2007 Model evaluation guidelines for systematic quantification of accuracy in watershed simulations. *Trans. ASABE* **50** (3), 885–900.

Mower, E. & Miranda, L. E. 2013 Frameworks for amending reservoir water management. *Lake Reservoir Manage.* **29** (3), 194–201.

Moy, W. S., Cohon, J. L. & ReVelle, C. S. 1986 A programming model for analysis of the reliability, resilience, and vulnerability of a water supply reservoir. *Water Resour. Res.* **22** (4), 489–498.

Muthuwatta, L. P., Ahmad, M. U. D., Bos, M. G. & Rientjes, T. H. 2010 Assessment of water availability and consumption in the Karkheh River Basin, Iran using remote sensing and geo-statistics. *Water Resour. Manage.* **24** (3), 459–484.

Nash, J. E. & Sutcliffe, J. V. 1970 River flow forecasting through conceptual models part I: a discussion of principles. *J. Hydrol.* **10** (3), 282–290.

Payne, J. T., Wood, A. W., Hamlet, A. F., Palmer, R. N. & Lettenmaier, D. P. 2004 Mitigating the effects of climate change on the water resources of the Columbia river basin. *Clim. Change* **62** (1), 233–256.

Pielke, R. A., Marland, G., Betts, R. A., Chase, T. N., Eastman, J. L., Niles, J. O., Niyogi, D. S. & Running, S. W. 2002 The influence of land-use change and landscape dynamics on the climate system: Relevance to climate-change policy beyond the radiative effect of greenhouse gases. In: *Capturing Carbon and Conserving Biodiversity – The Market Approach* (I. Swingland, ed.). Earthscan Publication, London, UK.

Pielke, R. A., Adegoke, J., Beltrán-Przekurat, A., Hiemstra, C. A., Lin, J., Nair, U. S., Niyogi, D. & Nobis, T. E. 2007 An overview of regional land-use and land-cover impacts on rainfall. *Tellus B Chem. Phys. Meteorol.* **59** (3), 587–601.

Polyakov, I. V. & Johnson, M. A. 2000 Arctic decadal and interdecadal variability. *Geophys. Res. Lett.* **27** (24), 4097–4100.

Prado, F. A., Athayde, S., Mossa, J., Bohlman, S., Leite, F. & Oliver-Smith, A. 2016 How much is enough? An integrated examination of energy security, economic growth and climate change related to hydropower expansion in Brazil. *Renew. Sustain. Energy Rev.* **53**, 1132–1136.

Sample, J. E., Duncan, N., Ferguson, M. & Cooksley, S. 2015 Scotland's hydropower: current capacity, future potential and the possible impacts of climate change. *Renew. Sustain. Energy Rev.* **52**, 111–122.

Schaefli, B., Hingray, B. & Musy, A. 2007 Climate change and hydropower production in the Swiss Alps: quantification of potential impacts and related modelling uncertainties. *Hydrol. Earth Syst. Sci. Discuss.* **11** (3), 1191–1205.

Shafiee, S. & Topal, E. 2009 When will fossil fuel reserves be diminished? *Energy Pol.* **37** (1), 181–189.

Singh, V. P., Khedun, C. P. & Mishra, A. K. 2014 Water, environment, energy, and population growth: implications for water sustainability under climate change. *J. Hydrol. Eng.* **19** (4), 667–673.

Sobhani, B., Eslahi, M. & Babaeian, I. 2016 Efficiency of statistical downscaling models of SDSM and LARS-WG in the simulation of meteorological parameters in Lake Urmia basin. *Phys. Geogr.* **47** (4), 1.

Sowers, J., Vengosh, A. & Weinthal, E. 2011 Climate change, water resources, and the politics of adaptation in the Middle East and North Africa. *Clim. Change* **104** (3), 599–627.

Srinivasan, K., Neelakantan, T. R., Narayan, P. S. & Nagarajukumar, C. 1999 Mixed-integer programming model for reservoir performance optimization. *J. Water Resour. Plan. Manage.* **125** (5), 298–301.

Taormina, R., Chau, K. W. & Sivakumar, B. 2015 Neural network river forecasting through baseflow separation and binary-coded swarm optimization. *J. Hydrol.* **529**, 1788–1797.

Teotónio, C., Fortes, P., Roebeling, P., Rodriguez, M. & Robaina-Alves, M. 2017 Assessing the impacts of climate change on hydropower generation and the power sector in Portugal: a partial equilibrium approach. *Renew. Sustain. Energy Rev.* **74**, 788–799.

Texas Commission on Environmental Quality 2007 *Water Availability Models: Rio Grande Basin.* Texas Commission on Environmental Quality, Austin, USA.

Van Vuuren, D. P., Edmonds, J., Kainuma, M., Riahi, K., Thomson, A., Hibbard, K., Hurtt, G. C., Kram, T., Krey, V., Lamarque, J. F. & Masui, T. 2011 The representative concentration pathways: an overview. *Clim. Change* **109** (1), 5–31.

Vicuña, S., Leonardson, R., Hanemann, M. W., Dale, L. L. & Dracup, J. A. 2008 Climate change impacts on high elevation hydropower generation in California's Sierra Nevada: a case study in the upper American river. *Clim. Change* **87**, 123–137.

Vörösmarty, C. J., Green, P., Salisbury, J. & Lammers, R. B. 2000 Global water resources: vulnerability from climate change and population growth. *Science* **289** (5477), 284–288.

Wang, W. C., Chau, K. W., Xu, D. M. & Chen, X. Y. 2015 Improving forecasting accuracy of annual runoff time series using ARIMA based on EEMD decomposition. *Water Resour. Manage.* **29** (8), 2655–2675.

Westaway, R. 2000 Modelling the potential effects of climate change on the Grande Dixence hydro-electricity scheme, Switzerland. *Water Environ. J.* **14** (3), 179–185.

Wilby, R. L. & Dawson, C. W. 2007 *SDSM 4.2: A Decision Support Tool for the Assessment of Regional Climate Change Impacts.* Department of Geography, Lancaster University, UK.

Wilby, R. L. & Harris, I. 2006 A framework for assessing uncertainties in climate change impacts: low-flow scenarios for the River Thames, UK. *Water Resour. Res.* **42** (2), W02419.

Wilby, R. L., Dawson, C. W. & Barrow, E. M. 2002 SDSM – A decision support tool for the assessment of regional climate change impacts. *Environ. Model. Softw.* **17** (2), 145–157.

Yip, S., Ferro, C. A., Stephenson, D. B. & Hawkins, E. 2011 A simple, coherent framework for partitioning uncertainty in climate predictions. *J. Clim.* **24** (17), 4634–4643.

Zarfl, C., Lumsdon, A. E., Berlekamp, J., Tydecks, L. & Tockner, K. 2015 A global boom in hydropower dam construction. *Aquat. Sci.* **77** (1), 161–170.

Zolghadr-Asli, B. 2017 Discussion of "Multiscale assessment of the impacts of climate change on water resources in Tanzania" by Umesh Adhikari, A. Pouyan Nejadhashemi, Matthew R. Herman, and Joseph P. Messina. *J. Hydrol. Eng.* **22** (8), 07017010.

Zolghadr-Asli, B., Bozorg-Haddad, O. & Loáiciga, H. A. 2016a Unionism and water resources management. *J. Irrig. Drain. Eng.* **143** (4), 02516003.

Zolghadr-Asli, B., Bozorg-Haddad, O. & Loáiciga, H. A. 2016b Time-based vulnerability: a step forward to operate water resources systems. *J. Irrig. Drain. Eng.* **142** (11), 02516001.

First received 22 May 2017; accepted in revised form 19 December 2017. Available online 2 February 2018